Shell Model Analysis of the Neutrinoless Double Beta Decay of ^{48}Ca

Mihai Horoi*
Department of Physics, Central Michigan University, Mount Pleasant, Michigan 48859, USA

Sabin Stoica
Horia Hulubei National Institute for Physics and Nuclear Engineering (IFIN-HH)
407 Atomistilor, Magurele-Bucharest 077125, Romania

(Dated: November 19, 2009)

The neutrinoless double beta ($0\nu\beta\beta$) decay process could provide crucial information to determine the absolute scale of the neutrino masses, and it is the only one that can establish whether neutrino is a Dirac or a Majorana particle. A key ingredient for extracting the absolute neutrino masses from $0\nu\beta\beta$ decay experiments is a precise knowledge of the nuclear matrix elements (NME) describing the half-life of this process. We developed a new shell model approach for computing the $0\nu\beta\beta$ decay NME, and we used it to analyze the $0\nu\beta\beta$ mode of ^{48}Ca. The dependence of the NME on the short range correlations parameters, on the average energy of the intermediate states, on the finite-size cutoff parameters, and on the effective interaction used for the many-body calculations is discussed.

PACS numbers: 23.40.Bw, 21.60.Cs, 23.40.-s, 14.60.Pq

arXiv:0911.3807v1 [nucl-th] 19 Nov 2009

I. INTRODUCTION

The neutrinoless double beta ($0\nu\beta\beta$) decay, which can only occur by violating the conservation of the total lepton number, if observed, will unravel physics beyond Standard Model (SM), and will represent a major milestone in the study of the fundamental properties of neutrinos [1]-[6]. Recent results from neutrino oscillation experiments have convincingly demonstrated that neutrinos have mass and they can mix [7]-[9]. The neutrinoless double beta ($0\nu\beta\beta$) decay is the most sensitive process to determine the absolute scale of the neutrino masses, and the only one that can distinguish whether neutrino is a Dirac or a Majorana particle. A key ingredient for extracting the absolute neutrino masses from $0\nu\beta\beta$ decay experiments is a precise knowledge of the nuclear matrix elements (NME) for this process. Since most of the $\beta\beta$ decay emitters are open shell nuclei, many calculations of the NME have been performed within the pnQRPA approach and its extensions [10]-[21]. However, the pnQRPA calculations are very sensitive to the variation of the so called g_{pp} parameter (the strength of the particle-particle interactions in the 1^+ channel) [10]-[12], and this drawback still persists in spite of various improvements brought by its extensions [13]-[18], including higher-order QRPA approaches [19]-[21]. The outcome of these attempts was that the calculations became more stable against g_{pp} variation, but at present there are still large differences between the values of the NME calculated with different QRPA-based methods, which do not yet provide a reliable determination of the two-neutrino double beta ($2\nu\beta\beta$) decay half-life. Therefore, although the QRPA methods do not seem to be suited to predict the $2\nu\beta\beta$ decay half-lives, one can use the measured $2\nu\beta\beta$ decay half-lives to calibrate the g_{pp} parameters that are further used to calculate the $0\nu\beta\beta$ decay NME [22]. Another method that recently provided NME for most $0\nu\beta\beta$ decay cases of interest is the Interactive Boson Model [23]. Given the novelty of these calculations, it remains to further validate their reliability by comparison with experimental data.

On the other hand, the progress in computer power, numerical algorithms, and improved nucleon-nucleon effective interactions, made possible large scale shell model calculations of the $2\nu\beta\beta$ and $0\nu\beta\beta$ decay NME [24]-[26]. The main advantage of the large scale shell model calculations is that they seem to be less dependent on the effective interaction used, as far as these interactions are consistent with the general spectroscopy of the nuclei involved in the decay. Their main drawback is the limitation imposed by the exploding shell model dimensions on the size of the valence space that can be used. The most important success of the large scale shell model calculations was the correct prediction of the $2\nu\beta\beta$ decay half-life for ^{48}Ca [24, 27]. In addition, these calculations did not have to adjust any additional parameters, i.e. given the effective interaction and the Gamow-Teller quenching factor extracted from the overall spectroscopy in the mass-region (including beta decay probabilities and charge-exchange form factors), one can reliably predict the $2\nu\beta\beta$ decay half-life of ^{48}Ca.

Clearly, there is a need to further check and refine these calculations, and to provide more details on the analysis of the NME that can be validated by experiments. We have recently revisited [28] the two neutrino double beta decay of ^{48}Ca using two recently proposed effective interactions for this mass region, GXPF1 and GXPF1A, and we explicitly analyzed the dependence of the double-Gamow-Teller sum entering the NME on the excitation

*Electronic address: horoi@phy.cmich.edu; URL: http://www.phy.cmich.edu/people/horoi

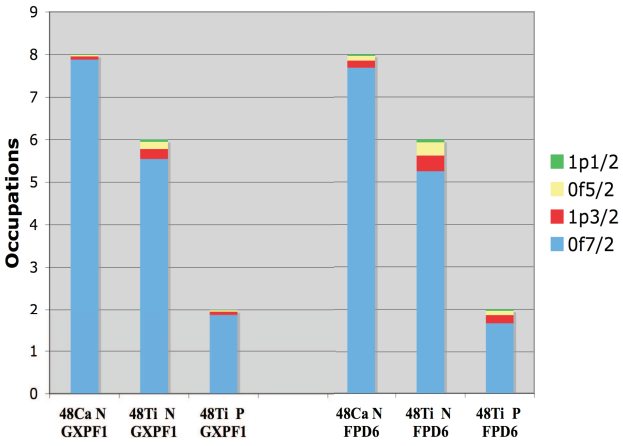

FIG. 1: (Color online) Comparison of the neutron and proton occupation probabilities between GXPF1 interaction and FPD6 interaction.

TABLE I: Neutron and proton occupation probabilities for the nuclei involved in the decay.

Nucleus (N/P)	Interaction	$0f_{7/2}$	$1p_{3/2}$	$0f_{5/2}$	$1p_{1/2}$
^{48}Ca N	GXPF1	7.883	0.073	0.033	0.011
^{48}Ti N	GXPF1	5.545	0.237	0.167	0.051
^{48}Ti P	GXPF1	1.846	0.110	0.033	0.011
^{48}Ca N	GXPF1A	7.892	0.067	0.032	0.009
^{48}Ti N	GXPF1A	5.535	0.248	0.168	0.048
^{48}Ti P	GXPF1A	1.839	0.119	0.032	0.010
^{48}Ca N	KB3	7.800	0.0706	0.105	0.024
^{48}Ti N	KB3	5.422	0.266	0.248	0.064
^{48}Ti P	KB3	1.770	0.120	0.089	0.022
^{48}Ca N	KB3G	7.795	0.070	0.112	0.024
^{48}Ti N	KB3G	5.416	0.260	0.263	0.061
^{48}Ti P	KB3G	1.763	0.120	0.097	0.021
^{48}Ca N	FPD6	7.693	0.161	0.117	0.029
^{48}Ti N	FPD6	5.253	0.369	0.310	0.068
^{48}Ti P	FPD6	1.673	0.196	0.101	0.031

energy of the 1^+ states in the intermediate nucleus ^{48}Sc. This sum was recently investigated experimentally [29], and it was shown that indeed, the incoherent sum (using only absolute values of the Gamow-Teller matrix elements) would provide an incorrect NME, validating our prediction. We have also corrected by several orders of magnitude the probability of transition of the g.s. of ^{48}Ca to the first excited 2^+ state of ^{48}Ti. Future experiments on double beta decay of ^{48}Ca (CANDLES [30] and CARVEL [31]) may reach the required sensitivity of measuring such transitions, and our results could be useful for planning these experiments.

In the present paper we continue our investigations of the double beta decay of ^{48}Ca, analyzing the $0\nu\beta\beta$ decay NME. ^{48}Ca has the largest $Q_{\beta\beta}$-value of 4.271 MeV (next largest is that of ^{150}Nd decay, 3.367 MeV), which could contribute to an increased decay probability. In addition, the high-energy gamma and beta radiation emitted in this process could help eliminate most of the background noise. However, the small natural abundance of this isotope, 0.187%, increases the difficulty of an experimental investigation, although new, improved separation techniques were recently proposed [32]. In addition, previous calculations [26, 33] suggest that its NME is a factor 4-5 smaller that those of other $\beta\beta$ emitters, such as ^{76}Ge and ^{82}Se [46]. Since these calculations were reported, it was shown that the short range correlations might not have such a dramatic effect on the NME [34, 35] as previously thought, and it was also shown that higher order terms in the nucleon currents could be important [35]. In the present paper we take into account all these new developments in the analysis of the NME for the $0\nu\beta\beta$ decay of ^{48}Ca, and we study the NME dependence on the short range correlations parameters, on the finite size parameter, on the average energy of the intermediate states, and on the effective interaction used for the many-body calculations.

II. THE NEUTRINOLESS DOUBLE BETA DECAY MATRIX ELEMENT

The $0\nu\beta\beta$ decay $(Z, A) \rightarrow (Z + 2, A) + 2e^-$ requires the neutrino to be a Majorana fermion, i.e. it is identical to the antineutrino. Considering only contributions from the light Majorana neutrinos [6], the $0\nu\beta\beta$ decay half-live is given by

$$\left(T^{0\nu}_{1/2}\right)^{-1} = G^{0\nu}_1 \mid M^{0\nu} \mid^2 \left(\frac{\langle m_{\beta\beta}\rangle}{m_e}\right)^2 , \qquad (1)$$

Here, $G^{0\nu}_1$ is the phase space factor, which depends on the $0\nu\beta\beta$ decay energy, $Q_{\beta\beta}$ and the nuclear radius. The effective neutrino mass, $\langle m_{\beta\beta}\rangle$, is related to the neutrino mass eigenstates, m_k, via the lepton mixing matrix, U_{ek},

$$\langle m_{\beta\beta}\rangle = \mid \sum_k m_k U^2_{ek} \mid \ . \qquad (2)$$

The NME, $M^{0\nu}$, is given by

$$M^{0\nu} = M^{0\nu}_{GT} - \left(\frac{g_V}{g_A}\right)^2 M^{0\nu}_F - M^{0\nu}_T \ , \qquad (3)$$

where $M^{0\nu}_{GT}$, $M^{0\nu}_F$ and $M^{0\nu}_T$ are the Gamow-Teller (GT), Fermi (F) and tensor (T) matrix elements, respectively. These matrix elements are defined as follows:

$$M^{0\nu}_\alpha = \sum_{m,n} \left\langle 0^+_f \mid \tau_{-m}\tau_{-n} O^\alpha_{mn} \mid 0^+_i \right\rangle \ , \qquad (4)$$

where O^α_{mn} are $0\nu\beta\beta$ transition operators, $\alpha = (GT,\ F,\ T)$, $\mid 0^+_i >$ is the g.s. of the parent

TABLE II: Parameters for the SRC parametrization of Eq. (11).

SRC	a	b	c
Miller-Spencer	1.10	0.68	1.00
CD-Bonn	1.52	1.88	0.46
AV18	1.59	1.45	0.92

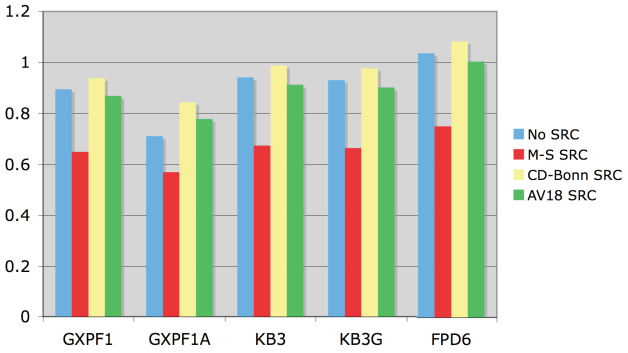

FIG. 2: (Color online) The dependence of the NME on the effective interaction used and the short range correlation (SRC) model. M-S stands for Miller-Spencer.

nucleus (in our case ^{48}Ca), and $\mid 0_i^+ >$ is the g.s. of the grand daughter nucleus (in our case ^{48}Ti).

Due to the two-body nature of the transition operator, the matrix element can be reduced to a sum of products of two-body transition densities TBTD and antisymmetrized two-body matrix elements,

$$M_\alpha^{0\nu} = \sum_{j_p j_{p'} j_n j_{n'} J_\pi} TBTD\left(j_p j_{p'}, j_n j_{n'}; J_\pi\right) \langle j_p j_{p'}; J^\pi T \mid \tau_{-1}\tau_{-2} O_{12}^\alpha \mid j_n j_{n'}; J^\pi T\rangle_a \ , \quad (5)$$

where O_{12}^α are given by

$$O_{12}^{GT} = \vec{\sigma}_1 \cdot \vec{\sigma}_2 H_{GT}(r) \ ,$$
$$O_{12}^{F} = H_F(r) \ ,$$
$$O_{12}^{T} = \left[3\left(\vec{\sigma}_1 \cdot \hat{r}\right)\left(\vec{\sigma}_1 \cdot \hat{r}\right) - \vec{\sigma}_1 \cdot \vec{\sigma}_2\right] H_T(r) \ . \quad (6)$$

The matrix elements of O_{12}^α for the jj-coupling scheme consistent with the conventions used by modern shell model effective interactions are described in the Appendix.

To calculate the two-body matrix elements in Eq. (5) one needs the neutrino potentials entering into the radial matrix element $\langle nl \mid H_\alpha \mid nl'\rangle$ in Eq. (13) below. Following Ref. [35] and using closure approximation one gets,

$$H_\alpha(r) = \frac{2R}{\pi}\int_0^\infty f_\alpha(qr)\frac{h_\alpha(q^2)}{q+\langle E\rangle} G_\alpha(q^2) q dq \ , \quad (7)$$

where $f_{F,GT}(qr) = j_0(qr)$ and $f_T(qr) = j_2(qr)$ are spherical Bessel functions, $\langle E\rangle$ is the average energy of the virtual intermediate states used in the closure approximation, and the form factors $h_\alpha(q^2)$ that include the higher order terms in the nucleon currents are

$$\begin{aligned} h_F(q^2) &= g_V^2(q^2) \\ h_{GT}(q^2) &= \frac{g_A^2(q^2)}{g_A^2}\left[1 - \frac{2}{3}\frac{q^2}{q^2+m_\pi^2} + \frac{1}{3}\left(\frac{q^2}{q^2+m_\pi^2}\right)^2\right] \\ &\quad + \frac{2}{3}\frac{g_M^2(q^2)}{g_A^2}\frac{q^2}{4m_p^2} \ , \\ h_T(q^2) &= \frac{g_A^2(q^2)}{g_A^2}\left[\frac{2}{3}\frac{q^2}{q^2+m_\pi^2} - \frac{1}{3}\left(\frac{q^2}{q^2+m_\pi^2}\right)^2\right] \\ &\quad + \frac{1}{3}\frac{g_M^2(q^2)}{g_A^2}\frac{q^2}{4m_p^2} \ . \end{aligned} \quad (8)$$

The $g_{V,A,M}$ form factors in Eq.(8) can include nucleon finite size effects, which in the dipole approximation are given by

$$\begin{aligned} g_V(q^2) &= \frac{g_V}{\left(1+q^2/\Lambda_V^2\right)^2}, \\ g_M(q^2) &= (\mu_p - \mu_n) g_V(q^2), \\ g_A(q^2) &= \frac{g_A}{\left(1+q^2/\Lambda_A^2\right)^2}. \end{aligned} \quad (9)$$

Here $g_V = 1$, $g_A = 1.25$, $(\mu_p - \mu_n) = 3.7$, $\Lambda_V = 850\ MeV$, and $\Lambda_A = 1086\ MeV$.

The short range correlations are included via the correlation function $f(r)$ that modifies the relative wavefunctions at short distances,

$$\psi_{nl}(r) \to \left[1 + f(r)\right]\psi_{nl}(r) \ , \quad (10)$$

where $f(r)$ can be parametrized as [35],

$$f(r) = -ce^{-ar^2}\left(1 - br^2\right) \ . \quad (11)$$

The radial matrix elements of H_α between relative harmonic oscillator wavefunctions $\psi_{nl}(r)$ and $\psi_{n'l'}(r)$, $\langle nl \mid H_\alpha(r) \mid n'l'\rangle$, become

$$\int_0^\infty r^2 dr \psi_{nl}(r) H_\alpha(r) \psi_{n'l'}(r)\left[1 + f(r)\right]^2 \quad (12)$$

TABLE III: Different contributions to the NME for the GXPF1A interaction with $\langle E\rangle = 7.72\ MeV$

SRC	$M_{GT}^{0\nu}$	$M_F^{0\nu}$	$M_T^{0\nu}$	$M^{0\nu}$
None	0.556	-0.219	-0.015	0.711
Miller-Spencer	0.465	-0.141	-0.014	0.570
CD-Bonn	0.688	-0.222	-0.014	0.845
AV18	0.634	-0.204	-0.014	0.779

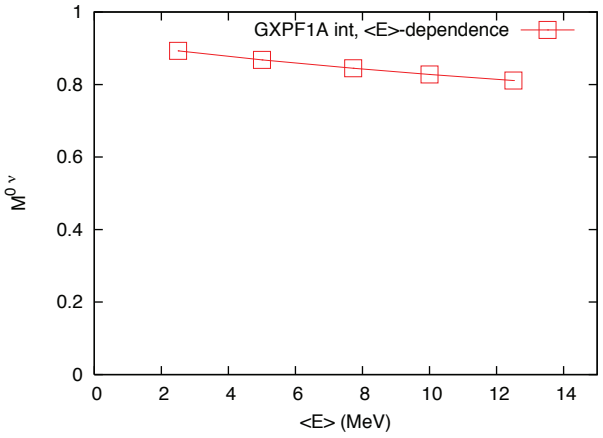

FIG. 3: (Color online) The dependence of the NME on the average energy of the intermediate states, $\langle E \rangle$, for the GXPF1A interaction.

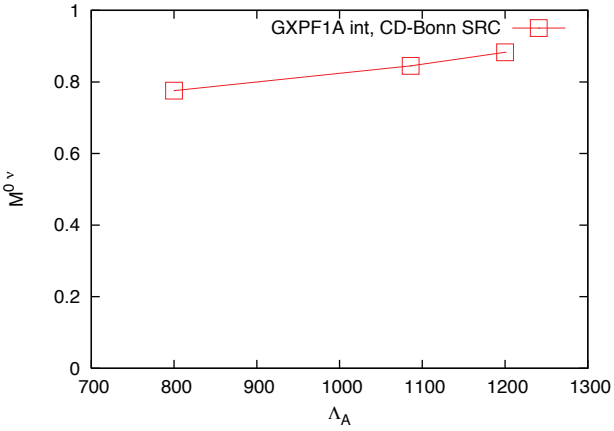

FIG. 4: (Color online) The dependence of the NME on the axial cutoff parameter Λ_A for the GXPF1A interaction.

Although the neutrino potentials are quite close to a Coulomb potential, the integrands in Eq. (7) are strongly oscillating, and the integrals require special numerical treatment.

Having calculated the two body matrix elements, we developed a new shell model approach for computing the many-body matrix elements for $0\nu\beta\beta$ transition, Eq. (5). This approach is briefly described in the Appendix.

III. RESULTS

In this study of the $0\nu\beta\beta$ decay NME we used five different effective interactions available for the shell model description of the pf-shell nuclei: GXPF1[36], GXPF1A [38], KB3 [39], KB3G [40], and FPD6 [41]. These effective interaction were constructed starting from a G-matrix [42] in the pf shell, which was further adjusted to describe some specific (but different) sets of experimental energy levels of some pf-shell nuclei. Although their elements are quite different, their predictions of the spectroscopic observables around A=48 are not very far apart. Recent experimental investigations [43, 44] of the nucleon occupation probabilities in ^{76}Ge and ^{76}Se and the subsequent theoretical analysis [35, 37] highlighted the relevance of these observables to obtain an accurate description of the nuclear structure of the nuclei involved in the double beta decay. Fig. 1 compares the neutron and proton occupation probabilities in ^{48}Ca and ^{48}Ti for two different effective interactions, GXPF1 and FPD6. One can see very small differences between the results of the two interactions. One can come to the same conclusion when comparing the similar occupations probabilities for all five interactions given in Table I.

In the present calculations we considered both short range correlation (SRC) effects and finite size (FS) effects. Although the radial dependence of the neutrino potential is very close to that of a Coulomb potential, many previous calculations [25, 26, 33, 46] took into account the SRC missing in the two-body product wave functions, via the Jastrow-like parametrization described in Eqs. (10)-(12). Until recently, the parameters a, b, c used were those proposed by Miller and Spencer [45], which have the effect of decreasing the NME by about 30%. Recently, [35] the SRC effects were revisited, using modern nucleon-nucleon interactions, such as CD-Bonn and AV18, and it was found that the decrease of the relative wave functions at short distances is compensated by a relative increase at larger distances, and the overall NME do not change very much when compared with the NME without SRC effects. Ref. [35] proposed a parametrization of these results in terms of similar Jastrow-like correlation functions as in Eq. (10)-(11), the corresponding parameters being listed in Table II. In addition, Ref. [34] introduced an effective $0\nu\beta\beta$ operator that takes into account the SRC effects and the contribution of the missing shells from the valence space using the general theory of effective interactions [42], and found that the NME for the $0\nu\beta\beta$ decay of ^{82}Se did not change significantly when compared with the result of the "bare" operator.

Fig. 2 shows our NME for all five effective interactions, for all three SRC set of parameters given in Table II, as well as for no SRC. One can see that the semi-quantitative analysis above is reflected in the dependence of NME on the choice of SRC. The results do not show significant dependence on the effective interaction used, although one can see a 20% spread of NME for the same choice of SRC. All NME reported here contain the higher order terms described in Eqs. (7)-(9). A comparison with the NME calculated without the higher order terms in the potential will be reported elsewhere. To be consistent [47] with the calculation of the phase factor, $G_1^{0\nu}$, we used $R = 1.2A^{1/3}\ fm$ in Eq. (7). Our choice for $\hbar\omega$ parameter entering the harmonic oscillator wave functions was $45A^{-1/3} - 25A^{-2/3}$, which was shown to provide better shell model description of observables than the simple

$41A^{-1/3}$ anstaz. Table III shows the GT, F, and T contributions to the overall NME for all SRC choices, when the GXPF1A interaction was used. One can see that all theses contributions add coherently in Eq. (3), and that the tensor contribution is negligible in all cases.

Fig. 3 shows the dependence of the NME of the average energy of the intermediate states. Varying $\langle E\rangle$ from 2.5 MeV to 12.5 MeV one gets less than 5% variation in the NME. This result suggests that closure approximation is quite good, although a direct study might be necessary to find out the exact magnitude of the error. All other NME results reported here used $\langle E\rangle = 7.72$ MeV. Fig. 4 shows the dependence of NME of the axial cutoff parameter Λ_A, while Λ_V is kept fixed at 850 MeV. The variation is within 5%, indicating a weak dependence of the FS cutoff parameters. The FS effects were implemented via the cutoff parameters Λ_V and Λ_A in the form factors given in Eq. (9). In most of our results, except those in Fig. 4, we use the same FS cutoff parameters as in Refs. [6, 35], i.e. $\Lambda_V = 850$ MeV and $\Lambda_A = 1086$ MeV. In Fig. 4 we present the dependence of the NME on Λ_A, while Λ_V is kept at its nominal value. As with the $\langle E\rangle$ dependence, the results varies by less than 5%.

IV. CONCLUSIONS AND OUTLOOK

In conclusion, we presented a new shell model analysis of the nuclear matrix elements for the neutrinoless double beta decay of ^{48}Ca. We included in the calculations the recently proposed higher order terms of the nucleon currents, three old and recent parametrization of the SRC effect, FS effects, intermediate states energy effects, and we treated careful few other parameters entering the into the calculations. We found very small variation of the NME with the average energy of the intermediate states, and FS cutoff parameters, and moderate variation vs the effective interaction and SRC parametrization. Our overall average NME using all values presented in Fig. 2 is 0.86, although the elimination of the Miller-Spencer SRC parametrization would significantly increase this value. We estimate the error due to the effects studied here to be about 18%. Using the present value of the NME and the recommended [47] phase-space factor $G_1^{0\nu} = 6.5\times10^{-14}\ yr^{-1}$ one can conclude that a future measurement of the $0\nu\beta\beta$ decay half-life of $10^{26}\ yr$, which seems to be the limit imposed by the present energy resolution of the CANDLES detector [32] (see also Fig. 21 of Ref. [48]), could detect a neutrino mass $\langle m_{\beta\beta}\rangle$ of about 230 ± 45 meV. New improvements in the detector technology could further reduce this limit.

We believe that our analysis covered the most important effects relevant to the accuracy of the NME for the double beta decay of ^{48}Ca. The successful prediction of the $2\nu\beta\beta$ decay half-live of ^{48}Ca using the shell model approach in the same model space suggests that the $0\nu\beta\beta$ decay half-life could be reliably predicted. Our analysis indicates that closure approximation is accurate at the level of 5% error. However, a direct comparison with the sum on intermediate states, calculated within the shell model, would be more reassuring.

As in all other $0\nu\beta\beta$ decay calculations reported so far, no quenching factors have been used. This is probably the least investigated potential effect on the $0\nu\beta\beta$ decay NME. It is possible that the GT-like operators be quenched even if they have finite range. No definitive conclusion exists about these effects, although Ref. [34] seems to indicate that they might not play a major role. One could try getting some insight into this problem by investigating the fictitious $0\nu\beta\beta$ decay of a light nucleus, such as ^{16}Be, and increasing the valence space one can study the changes of different contributions to the NME.

V. APPENDIX

The matrix element of O_{12}^{α} for non-antisymmetrized jj-coupling two-particle states can be decomposed into products of reduced matrix elements of the spin, relative and center of mass operators,

$$\begin{aligned}
&\langle n_1 l_1 j_1, n_2 l_2 j_2; J^\pi T=1 \mid O_{12}^{\alpha} \mid n_1' l_1' j_1', n_2' l_2' j_2'; J^\pi T=1\rangle = \\
&\sum_{S\lambda} \left\langle l_1 \frac{1}{2}(j_1), l_2 \frac{1}{2}(j_2) \mid \frac{1}{2}\frac{1}{2}(S), l_1 l_2(\lambda)\right\rangle_J \left\langle l_1' \frac{1}{2}(j_1'), l_2' \frac{1}{2}(j_2') \mid \frac{1}{2}\frac{1}{2}(S), l_1' l_2'(\lambda)\right\rangle_J \frac{1}{\sqrt{(2S+1)}} \left\langle \frac{1}{2}\frac{1}{2}; S \| S_\alpha^{(0)} \| \frac{1}{2}\frac{1}{2}; S\right\rangle \\
&\times \sum_{nn'lNL} \langle nl, NL \mid n_1 l_1, n_2 l_2\rangle_\lambda \langle n' l, NL \mid n_1' l_1', n_2' l_2'\rangle_\lambda \langle nl \mid H_\alpha(r) \mid n' l\rangle \,. \qquad (13)
\end{aligned}$$

where

$$\left\langle l_1 \frac{1}{2}(j_1), l_2 \frac{1}{2}(j_2) \mid \frac{1}{2}\frac{1}{2}(S), l_1 l_2(\lambda)\right\rangle_J = \sqrt{(2j_1+1)(2j_2+1)(2S+1)(2\lambda+1)} \begin{pmatrix} l_1 & \frac{1}{2} & j_1 \\ l_2 & \frac{1}{2} & j_2 \\ \lambda & S & J \end{pmatrix} , \qquad (14)$$

and the last factor is a 9j symbol. As mentioned in the text, the order of the spin-orbit coupling must be consistent with the convention considered into the derivation

of the effective interaction used for the many body calculations ($\vec{l}+\vec{s}$ in most cases). The reduced spin matrix elements are

$$\left\langle \frac{1}{2}\frac{1}{2}S\|\vec{\sigma}_1\cdot\vec{\sigma}_2\|\frac{1}{2}\frac{1}{2}S\right\rangle = \sqrt{2S+1}\,[2S(S+1)-3]\ ,$$
$$\left\langle \frac{1}{2}\frac{1}{2}S\|1\|\frac{1}{2}\frac{1}{2}S\right\rangle = \sqrt{2S+1}\ . \quad (15)$$

The expressions for the matrix elements of the tensor operator will be given elsewhere. Our calculations show that the tensor term gives a small contribution to the NME in most cases. The higher order terms in the nucleon currents, however, decrease the overall NME by about 20-25%. The antisymmetrized form of the two-body matrix elements can be obtained using

$$\langle j_p j_{p'};J^\pi T \mid t_{-1}t_{-2}O^\alpha_{12} \mid j_n j_{n'};J^\pi T\rangle_a = \frac{1}{\sqrt{(1+\delta_{j_p j'_{p'}})(1+\delta_{j_n j_{n'}})}}\times [\langle j_p j_{p'};J^\pi T \mid t_{-1}t_{-2}O^\alpha_{12} \mid j_n j_{n'};J^\pi T\rangle - (-1)^{j_n+j_{n'}+J}\langle j_p j_{p'};J^\pi T \mid t_{-1}t_{-2}O^\alpha_{12} \mid j_{n'} j_n;J^\pi T\rangle] \quad (16)$$

Having the two-body matrix elements ready, one can calculate the NME in Eq. (5) if two body transition densities $TBTD\,(j_p j_{p'}, j_n j_{n'}; J_\pi)$ are known. Most of the shell model codes do not provide two body transition densities. One alternative approach is to take advantage of the isospin symmetry that most of the effective interactions have, which creates wave functions with good isospin. The approach described below works also when the proton and neutron are in different shells. If the above conditions are satisfied, one can transform the two body matrix elements of a $\Delta T = 2$ operator using the Wigner-Eckart theorem, from $\Delta T_z = -2$ to $\Delta T_z = 0$, which can be further used (see below) to describe transitions between states of the same nucleus. Denoting

$$\left\langle O^{\Delta T=2}_{\Delta T_z=-2}\right\rangle = \quad (17)$$
$$\left\langle T=1\ T_z=-1 \mid O^{\Delta T=2}_{\Delta T_z=-2} \mid T=1\ T_z=1\right\rangle, \quad (18)$$

one gets for the $\Delta T_z = 0$ the two body matrix elements

$$< pp \mid O^{\Delta T=2}_{\Delta T_z=0} \mid pp >=$$
$$< nn \mid O^{\Delta T=2}_{\Delta T_z=0} \mid nn >=$$
$$< O^{\Delta T=2}_{\Delta T_z=-2} > \times C^{1\ 2\ 1}_{1\ 0\ 1}/C^{1\ \ 2\ \ 1}_{1\ -2\ -1}, \quad (19)$$

and

$$< pn\ T=1 \mid O^{\Delta T=2}_{\Delta T_z=0} \mid pn\ T=1 >=$$
$$< O^{\Delta T=2}_{\Delta T_z=-2} > \times C^{1\ 2\ 1}_{0\ 0\ 0}/C^{1\ \ 2\ \ 1}_{1\ -2\ -1}, \quad (20)$$

where $C^{1\ \ 2\ \ 1}_{T_{zi}\ \Delta T_z\ T_{sf}}$ are isospin Clebsch-Gordan coefficients. The transformed matrix elements in Eqs. (19) and (20) preserve spherical symmetry and they can be used as a piece of a Hamiltonian, $H^\alpha_{\beta\beta}$, that violates isospin symmetry.

One can then lower by 2 units the isospin projection of the g.s. of the parent nucleus that has the higher isospin $T_>$, ^{48}Ca in our case, thus becoming an isobar analog state of the grand daughter nucleus that has isospin $T_< = T_> - 2$, ^{48}Ti in our case. Denoting by $\mid 0^+_{i<}\ T_> >$ the transformed state, one can now calculate the many body matrix elements of the transformed $0\nu\beta\beta$ operator,

$$M^{0\nu}_\alpha(T_z=T_<) = \left\langle 0^+_f\ T_< \mid H^\alpha_{\beta\beta} \mid 0^+_{i<}\ T_>\right\rangle. \quad (21)$$

Choosing $\mid 0^+_{i<}\ T_> >$ as a starting Lanczos vector, and performing one Lanczos iteration with $H^\alpha_{\beta\beta}$ one gets

$$H^\alpha_{\beta\beta} \mid 0^+_{i<}\ T_> >= a_1 \mid 0^+_{i<}\ T_> > + b_1 \mid L_1 >, \quad (22)$$

where $\mid L_1 >$ is the new Lanczos vector. Then, one can calculate the matrix elements in Eq. (21)

$$M^{0\nu}_\alpha(T_z=T_<) = b_1 \left\langle 0^+_f\ T_< \mid L_1\right\rangle. \quad (23)$$

The transition matrix elements in Eq. (5) can then be recovered using again the Wigner-Eckart theorem,

$$M^{0\nu}_\alpha = M^{0\nu}_\alpha(T_z=T_<)\times C^{T_>\ \ 2\ T_<}_{T_>\ -2\ T_<}/C^{T_>\ 2\ T_<}_{T_<\ 0\ T_<}. \quad (24)$$

Although it looks complicated, this procedure is rather easy to implement. The transformation of the g.s. of the parent to an analog state of the grand daughter can be performed very quickly, and one Lanczos iteration represents a small load as compared with the calculation of the g.s. of the grand daughter. The additional calculations described in Eqs. (22)-(24) require smaller resources than those necessary to calculate the TBTDs.

Acknowledgments

M.H. acknowledges support from NSF Grant No. PHY-0758099.

[1] W.C. Haxton and G.J. Stephenson, Prog. Part. Nucl. Phys. **12**, 409 (1984).

[2] J. Suhonen and O. Civitarese, Phys. Rep. **300**, 123

(1998).
[3] A. Faessler and F. Simkovic, J. Phys. G: Nucl. Part. Phys. **24**, 2139 (1998).
[4] H.V. Klapdor-Kleingrothaus, "60 Years of Double-Beta Decay - From Nuclear Physics to Beyond Standard Model Particle Physics", World Scientific, Singapore, 2001.
[5] S.R. Elliot and P. Vogel, Annu. Rev. Nucl. Part. Sci. **52**, 115 (2002).
[6] F.T. Avignone, S.R. Elliot, and J. Engel, Rev. Mod. Phys. **80**, 481 (2008).
[7] B. Aharmim et al., Phys. Rev. C **72**, 055502 (2005).
[8] C. Arsepella et al., Phys. Lett. B **658**, 101 (2008); T. Araki et al., Phys. Rev. Lett. **94**, 081801 (2005).
[9] T. Schwetz, Nucl. Phys. B (proc. Suppl) **188**, 158 (2008).
[10] P. Vogel and M. R. Zirnbauer, Phys. Rev. Lett. **57**, 3148 (1986).
[11] K. Grotz and H.V. Klapdor, Nucl. Phys. **A 460**, 395 (1986).
[12] J. Suhonen, T. Taigel and A. Faessler, Nucl. Phys. **A 486**, 91 (1988).
[13] A. Staudt, K. Muto and H.V. Klapdor-Kleingrothaus, Europhys. Lett. **13**, 31 (1990).
[14] O. Civitarese, A. Faessler, J. Suhonen, X.R. Wu, Phys. Lett. B **251**, 333 (1990).
[15] S. Stoica and W.A. Kaminski, Phys. Rev.**C 47**, 867 (1993); S. Stoica, Phys. Rev. **C 49**, 2240 (1994); S. Stoica, Phys. Lett. **B 350**, 152 (1995); S. Stoica and I. Mihut, Nucl. Phys. **A 602** (1996); S. Stoica and H.V. Klapdor-Kleingrothaus, Nucl. Phys.**A 694**, 269 (2001).
[16] A.A. Raduta, D.S. Delion, A. Faessler, Phys. Rev. C **51**, 3008 (1995).
[17] G. Pantis, F. Simkovic, J.D. Vergados, A. Faessler, Phys. Rev. C **53**, 695 (1996).
[18] A. Bobyk, W.A. Kaminski and P. Zareba, Eur. Phys. J. **A 5**, 385 (1999); Nucl. Phys. **A669**, 221 (2000).
[19] A. A. Raduta, A. Faessler, S. Stoica and W. A. Kaminski, Phys. Lett. **B 254**, 7 (1991);
A.A. Raduta, A. Faessler and S. Stoica, Nucl. Phys. **A 534**, 149 (1991).
[20] J. Toivanen and J. Suhonen, Phys. Rev. Lett. **75**, 410 (1995); Phys. Rev. **C 55**, 2314 (1997).
[21] F. Simkovic, J. Schwieger, M. Veselsky, G. Pantis, A. Faessler, Phys. Lett. **393**, 267 (1997).
[22] V. A. Rodin, A. Faessler, F. Simkovic, and P. Vogel, Nucl. Phys. **A766**, 107 (2006), erratum ibidem.
[23] J. Barea and F. Iachello, Phys. Rev. C **79**, 044301 (2009).
[24] E. Caurier, A. Poves, and A.P. Zuker, Phys. Lett. **B252**, 13 (1990).
[25] E. Caurier, F. Nowacki, A. Poves and J. Retamosa, Phys. Rev. Lett. **77**, 1954 (1996).
[26] J. Retamosa, E. Caurier, F. Nowacki, Phys. Rev. **C 51**, 371 (1995).
[27] A. Balysh, A. De Silva, V. I. Lebedev, K. Lou, M. K. Moe, M. A. Nelson, A. Piepke, A. Pronskiy, M. A. Vient, and P. Vogel, Phys. Rev. Lett. **77**, 5186 (1996).
[28] M. Horoi, S. Stoica, B.A. Brown, Phys Rev **C 75** 034303 (2007)
[29] K. Yako, et al., Phys. Rev. Lett. **103**, 012503 (2009).
[30] S. Umehara, et al., Journal of Physics: Conference Series **39**, 356358 (2006).
[31] Yu. G. Zdesenko, et al., Astropart. Phys. **23**, 249 (2005).
[32] I. Ogawa, "CANDLES for the study of ^{48}Ca double beta decay", Bull. Amer. Phys. Soc., Vol. **54**, No. 10., page 19 (2009).
[33] A. Poves, E. Caurier, and F. Nowacki, e-print arXiv:0709.0277 (2007).
[34] J. Engel and G. Hagen, Phys. Rev. C **79**, 064317 (2009).
[35] F. Simkovic, A. Faessler, H. Muther, V. Rodin, and M. Stauf, Phys. Rev. C **79**, 055501 (2009).
[36] M. Honma, T. Otsuka, B.A. Brown, and T. Mizusaki, Phys. Rev. C **69**, 034335 (2004).
[37] J. Menendez, A. Poves, E. Caurier, and F. Nowacki, Phys. Rev. C **80**, 048501 (2009).
[38] M. Honma, T. Otsuka, B.A. Brown, and T. Mizusaki, Eur. Phys. J. A **25** Suppl. 1, 499 (2005).
[39] A. Poves and A.P.Zuker, Phys. Rep. **71**, 141 (1981).
[40] A. Poves et al., Nucl. Phys. **A694**, 157 (2001).
[41] W. A. Richter, M. G. van der Merwe, R. E. Julies, and B. A. Brown, Nucl. Phys. **A523**, 325 (1991).
[42] M. Hjorth-Jensen, T. T. S. Kuo and E. Osnes, Phys. Rep. **261**, 125 (1995).
[43] J. Schiffer et al., Phys. Rev. Lett. **100**, 112501 (2008).
[44] B.P. Kay et al., Phys. Rev. C **79**, 021301(R) (2009).
[45] G. A. Miller and J. E. Spencer, Ann. Phys. (NY) **100**, 562 (1976).
[46] E. Caurier, J. Menendez, F. Nowacki, and A. Poves, Phys. Rev. Lett. **100**, 052503 (2008).
[47] S. Cowell, Phys. Rev. C **73**, 028501 (2006).
[48] F. T. Avignone III, G. S. King III, and Yu. G. Zdesenko, New Journal of Physics **7**, 6 (2005).